Fast Inactivation of Delayed Rectifier K Conductance in Squid Giant Axon and Its Cell Bodies

Chris Mathes,* Joshua J.C. Rosenthal,* Clay M. Armstrong,‡ and William F. Gilly*

From the *Hopkins Marine Station, Department of Biological Sciences, Stanford University, Pacific Grove, California 93950; and ‡Department of Physiology, University of Pennsylvania, Philadelphia, Pennsylvania 19104

ABSTRACT Inactivation of delayed rectifier K conductance (g_K) was studied in squid giant axons and in the somata of giant fiber lobe (GFL) neurons. Axon measurements were made with an axial wire voltage clamp by pulsing to V_K (~ -10 mV in 50–70 mM external K) for a variable time and then assaying available g_K with a strong, brief test pulse. GFL cells were studied with whole-cell patch clamp using the same prepulse procedure as well as with long depolarizations. Under our experimental conditions (12–18°C, 4 mM internal MgATP) a large fraction of g_K inactivates within 250 ms at -10 mV in both cell bodies and axons, although inactivation tends to be more complete in cell bodies. Inactivation in both preparations shows two kinetic components. The faster component is more temperature-sensitive and becomes very prominent above 12°C. Contribution of the fast component to inactivation shows a similar voltage dependence to that of g_K, suggesting a strong coupling of this inactivation path to the open state. Omission of internal MgATP or application of internal protease reduces the amount of fast inactivation. High external K decreases the amount of rapidly inactivating I_K but does not greatly alter inactivation kinetics. Neither external nor internal tetraethylammonium has a marked effect on inactivation kinetics. Squid delayed rectifier K channels in GFL cell bodies and giant axons thus share complex fast inactivation properties that do not closely resemble those associated with either C-type or N-type inactivation of cloned Kv1 channels studied in heterologous expression systems.

KEY WORDS: nerve • channels • voltage clamp • phosphorylation • temperature

INTRODUCTION

Functional properties of the diverse array of voltage-dependent K channels are important determinants of electrical excitability in many cells (Rudy, 1988). Numerous K channel α-subunits have now been molecularly identified, and their functional properties have been extensively studied in heterologous expression systems (Jan and Jan, 1992; Pongs, 1992). It remains problematic, however, to correlate molecular, biochemical, and physiological properties of specific K channels expressed in native cells or in specific cellular domains, such as the cell body and axon of individual neurons.

Squid giant axon and its cell bodies in the giant fiber lobe (GFL)[1] of the stellate ganglion provide an attractive system for carrying out such work. Cell bodies and giant axons can be selectively studied physiologically and biochemically, and the complement of K channel subtypes is relatively simple. The major portion of macroscopic K conductance (g_K) in the GFL/giant axon system is due to a 20-pS channel (Llano and Bookman, 1986; Perozo et al., 1991; Nealey et al., 1993), and this delayed rectifier g_K has been extensively studied. Only two other minor K channel species (10 pS and 40 pS) have been reported (Llano et al., 1988; Nealey et al., 1993).

Activation properties of the 20-pS channels are similar in axons and cell bodies (Llano and Bookman, 1986; Nealey et al., 1993), but the picture is less clear for inactivation. Macroscopic g_K in GFL cell bodies partially inactivates with a time constant of <100 ms at 10–12°C, and this property is shared by the somatic 20-pS channel (Llano and Bookman, 1986). Delayed rectifier g_K in giant axon, on the other hand, is generally thought to show no fast inactivation (Keynes, 1994), and single channel recordings of axonal 20-pS channels have not been focused on this issue (Llano et al., 1988; Perozo et al., 1991).

In reality, few studies have specifically looked for fast inactivation in giant axons, and such experiments in perfused axons are complicated by technical difficulties. Depolarizations that produce outward K current (I_K) result in K accumulation in the extracellular space and a change in driving force (Frankenhaeuser and Hodgkin, 1956). In addition, the axial wire polarizes during long pulses and can lead to inadequate voltage control (Hodgkin and Huxley, 1952*a*). Both problems produce a decline of I_K during a pulse that superficially resembles inactivation. These errors can be circumvented by studying inactivation in high external K (Ehrenstein and Gilbert, 1966) and at a voltage equal

Address correspondence to Dr. William F. Gilly, Hopkins Marine Station, Stanford University, Pacific Grove, CA 93950. Fax: 408-655-6220; E-mail: Lignje@leland.stanford.edu

[1]*Abbreviation used in this paper:* GFL, giant fiber lobe.

to the K channel reversal potential (V_K). This approach showed that axonal g_K inactivates with a complex time-course, but no inactivation was detected before 100 ms at voltages up to −10 mV (Clay, 1989; see also Chabala, 1984).

Recently we described similar experiments which revealed that axonal and somatic g_K inactivate in a comparable manner and proposed that a single type of 20-pS channel constitutes the delayed rectifier in axons and in cell bodies (Rosenthal et al., 1996). In this paper we present a more complete analysis of g_K inactivation in the GFL/giant axon system. A fast phase of inactivation is very dependent on temperature and the presence of internal ATP. A prominent slower component of inactivation is relatively insensitive to these agents. Complex inactivation kinetics that are susceptible to modification are thus characteristic of squid delayed rectifier g_K.

METHODS

Recordings from GFL Neurons

Adult *Loligo opalescens* were collected from Monterey Bay and maintained in flow-through seawater at ambient temperature (~15°C). Somata of GFL neurons were isolated from the posterior tip of the stellate ganglion and cultured at 16°C as described elsewhere (Gilly et al., 1990). Cells were normally used for recording within 2 d of isolation.

Conventional, whole-cell patch clamp was employed (Gilly et al., 1990). Effective series resistance after electronic compensation was estimated by analyzing capacity current transients for a 10-mV step (Armstrong and Gilly, 1992) and ranged from 0.2 to 0.8 MΩ. Holding potential was −80 mV throughout, and linear capacity and ionic currents were removed on-line with a standard P/−4 technique. Filtering was at 10 kHz; sampling was carried out at either 20 or 2 kHz.

The internal solution (150 K_i) was similar to the perfusate used for giant axons (see below) and contained (in mM): 20 KCl, 80 K glutamate, 50 KF, 10 lysine (titrated to pH 7.0 with HEPES), 1 EGTA, 1 EDTA, 381 glycine, 291 sucrose, 4 Mg ATP, and 5 TMA OH (pH 7; 966 mosm). The standard external solution (20 K_o) contained (in mM): 20 KCl, 480 NaCl, 10 $MgCl_2$, 10 $CaCl_2$, 10 $MgSO_4$, 10 HEPES, and 0.0002 TTX (pH 7.7; 980 mosm). In some cases, higher external K was used, and Na was reduced on an equimolar basis (see appropriate figure legends). Experiments described in conjunction with Fig. 5 used slightly different external and internal solutions whose compositions are given in the figure legend. Junction potentials of ~−10 mV exist between the internal and external solutions and have been ignored. Tityustoxin-K_α was a gift from Drs. M.P. Blaustein and D.R. Matteson, University of Maryland (Baltimore, MD).

Recordings from Giant Axons

Adult squid (*L. pealei*) were supplied by the Marine Biological Laboratory, Woods Hole, MA during July 1995 and maintained at 14°C. Cleaned giant axons were studied with a conventional axial-wire voltage clamp (Gilly and Armstrong, 1982) following internal perfusion with (in mM): 50 or 70 KF, 10 HEPES, 1 EGTA, 1 EDTA, 450 glycine, 450 sucrose, 3 lysine, 4 Mg ATP, and 4 TMA OH (pH 7.2; 980 mosm). The standard external solution con-

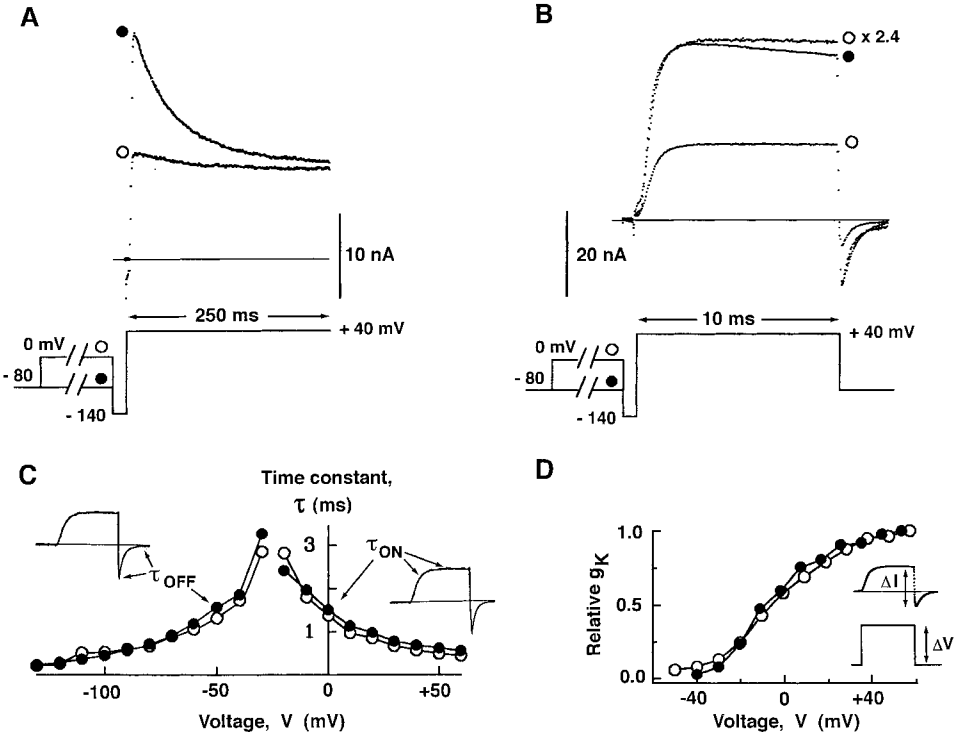

FIGURE 1. Activation properties of inactivating and noninactivating I_K in GFL neurons are similar. (*A*) I_K recorded at +40 mV with (○) and without (●) a 500-ms prepulse to 0 mV. Test pulses were preceded by a 5-ms period at −140 mV to close channels that were open at the end of the prepulse. Inactivating I_K is greatly reduced, but steady-state I_K is not much affected. (*B*) I_K during a short pulse recorded with (○) and without (●) the same prepulse procedure as in *A*. Comparison of activation kinetics is facilitated by scaling the prepulse-resistant I_K trace by a factor of 2.4. (*C*) Voltage dependence of activation and deactivation kinetics is not altered by an inactivating prepulse. Values for activation (τ_{ON}) and deactivation (τ_{OFF}) were obtained by fitting single exponentials to I_K recorded with (○) and without (●) the prepulse in *A*. τ_{ON} was fit to the final 25% approach to peak I_K; τ_{OFF} was fit to the entire tail current following repolarization from a strong, brief pulse (see *inset*). (*D*) Steady-state voltage dependence of g_K is not altered by the inactivating prepulse. g_K was determined as $\Delta I/\Delta V$ (see *inset*) from I_K traces recorded with (○) and without (●) the prepulse in *A*. (18°C, 20 K_o//150 K_i, 5 d in vitro.)

tained (in mM): 50 or 70 KCl, 380 or 360 NaCl, 38 $CaCl_2$, 14 $MgSO_4$, 10 HEPES, and 0.0002 TTX (pH 7.2; 980 mosm). Junction potentials were ignored. Unfiltered data were sampled at 50 kHz.

RESULTS

Properties of Inactivating and Noninactivating K Conductance in GFL Neurons

Results in this paper are developed around the idea that a single type of K channel underlies delayed rectifier g_K in both squid giant axons and cell bodies of GFL neurons. Logic behind this assertion is summarized above, and additional arguments are presented elsewhere (Horrigan and Gilly, 1996). Identification of the cDNA SqKv1A also supports this idea (Rosenthal et al., 1996). SqKv1A mRNA is expressed in GFL neurons and appears to encode both somatic and axonal K channel protein, and injection of cRNA into *Xenopus* oocytes produces K channels with appropriate functional properties. Regardless of whether SqKv1A α subunits are expressed in frog oocytes, squid axons, or GFL cell bodies, inactivation is incomplete.

Results in Fig.1 indicate that the K channels underlying inactivating and noninactivating I_K in GFL neurons share important biophysical properties. A 500-ms prepulse to 0 mV produces a decrease in peak I_K of ~50% but has almost no effect on steady-state I_K (Fig. 1 *A*). We consider the prepulse-resistant I_K (○) to be essentially noninactivating on this time-scale. Fig. 1 *B* illustrates corresponding I_K traces obtained at higher sampling rate. Scaling the prepulse-resistant trace (○) by a factor of 2.4 shows that noninactivating I_K and total I_K have indistinguishable activation and deactivation kinetics. This comparison between total and noninactivating I_K was carried out over a range of activation (ON) and deactivation (OFF) voltages (Fig. 1 *C*), and single exponentials were fit to determine τ_{ON} and τ_{OFF} as indicated in the insets. Fig. 1 *D* shows that the normalized g_K-voltage relationships are also indistinguishable. Thus, fundamental activation properties of inactivating and noninactivating K channels in GFL neurons appear to be identical, consistent with a single population of channels that inactivate incompletely.

Fig. 2 provides pharmacological support for this idea. Tityustoxin-K_α is a scorpion polypeptide that blocks certain mammalian K channels (Werkman et al., 1993), and its effect on I_K in a GFL neuron is illustrated in Fig. 2, *A* and *B*. 300 nM tityustoxin reversibly reduces peak and steady-state I_K by a comparable factor with little effect on kinetics. Tityustoxin also blocks I_K in giant axons during brief pulses (data not illustrated), but long pulses were not studied.

Similar results in GFL cells were produced by high concentrations of external TEA (Fig. 2, *C* and *D*). Internal TEA blocks I_K at much lower concentrations, but also produces no major kinetic alteration. Records in Fig. 2, *E* and *F* were obtained 1 min and 18 min after achieving the whole-cell configuration with 1.6 mM TEA in the pipette. Results with all three ways of blocking I_K are thus consistent with a single type of channel underlying the delayed rectifier g_K in GFL cells.

The fact that neither internal nor external TEA produces a strong effect on inactivation kinetics in GFL cells is unusual, because TEA is known to compete with both N-type (intracellular) and C-type (extracellular) inactivation in cloned Kv1 channels (Choi et al., 1991). More subtle effects of external TEA on inactivation kinetics in GFL cells are described below.

Inactivation Kinetics in GFL Neurons and in Giant Axons

Fig. 3 *A* illustrates the procedure used to study inactivation kinetics in this study and raw data from a GFL neuron. Each prepulse to −10 mV of varying duration (Δt)

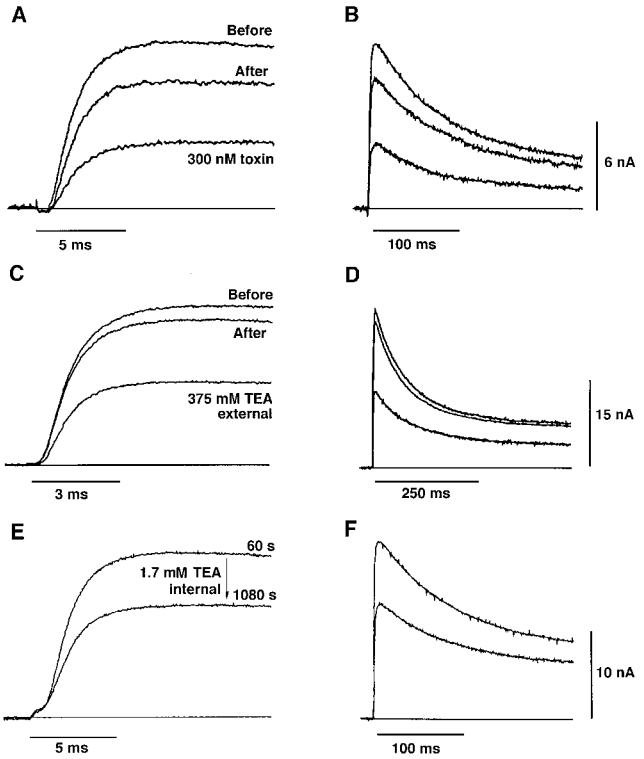

FIGURE 2. Inactivating and noninactivating I_K in GFL neurons share pharmacological sensitivities. (*A* and *B*) I_K traces were recorded for short (*A*) and long pulses (*B*) to +40 mV before addition of toxin, after 6 min exposure to 300 nM tityustoxin-K_α, and 130 min after wash-out of the toxin. Both peak and steady-state I_K are comparably reduced by tityustoxin. The small inward currents before the onset of I_K are Ca currents that do not inactivate that are present to a variable degree in GFL cells (McFarlane and Gilly, 1996). (12°C, 20 K_o (pH 8.6)//150 K_i.) (*C* and *D*) Similar results were obtained with externally applied 375 mM TEA-Cl. (18°C, 5 K_o//150 K_i.) (*E* and *F*) Internal TEA does not alter appreciably alter I_K kinetics at +40 mV. I_K traces of larger amplitude were recorded ~60 s after achieving the whole-cell configuration with 1.7 mM TEA in the pipette, and the smaller amplitude traces were obtained ~1,000 s later. (12°C, 20 K_o//150 K_i + 1.7 TEA.)

was followed by a strong test pulse to determine the amount of available I_K (I(Δt)). Maximal I_K occurs with a short prepulse (Δt = 1.6 ms), and longer prepulses produce progressively smaller I_K due to developing inactivation. Values of I(Δt)/I(1.6 ms) from this procedure are compared in Fig. 3 *B* (●) to a record of I_K directly recorded at −10 mV after scaling so that I (1.6 ms) = peak I_K (−10 mV).

Fig. 3 *C* establishes the time course at which the inactivating portion of I_K declined at −10 mV in the prepulse experiment (noninactivating I_K was subtracted out, see legend). Inactivation kinetics can be described by the sum of two exponentials (*solid curve*) whose amplitudes and time constants were obtained by simultaneous fitting. Fast (τ_F) and slow (τ_S) time constants are 55 and 277 ms; the corresponding fractional amplitudes are 0.77 (A_F) and 0.25 (A_S). Inactivation thus has fast and slow components operating on time scales of tens and hundreds of ms, respectively.

Application of the same prepulse procedure to a giant axon reveals similar fast and slow components of inactivation. Fig. 3 *D* shows I(Δt) records for three different prepulses to −7 mV, which was identified as the reversal potential (V_K) for I_K tails following a brief pulse (0.5 ms to +60 mV). Normalized peak amplitude of I(Δt) from this experiment is plotted versus prepulse duration in Fig. 3 *E* (○), along with the value of current at the end of each prepulse (◆). Zero current flow during the prepulse indicates that V_K did not change during the measurements, and deviation of V_K from its original value was estimated to be <-2 mV in this experiment.

These data demonstrate that the large decline in I(Δt) in Fig. 3 *E* is an inactivation process analogous to that in GFL neurons. Kinetics of inactivation in this axon are further analyzed in Fig. 3 *F*. Fast and slow components are evident, and the solid curve is the sum of two exponentials with time constants (τ_F = 62 ms, τ_S = 447 ms) and amplitudes (A_F = 0.67, A_S = 0.34) comparable to those derived from GFL data (dashed curve is replotted fit from Fig. 3 *C*).

Results thus obtained from a number of GFL neurons and giant axons are compared in Table I. Al-

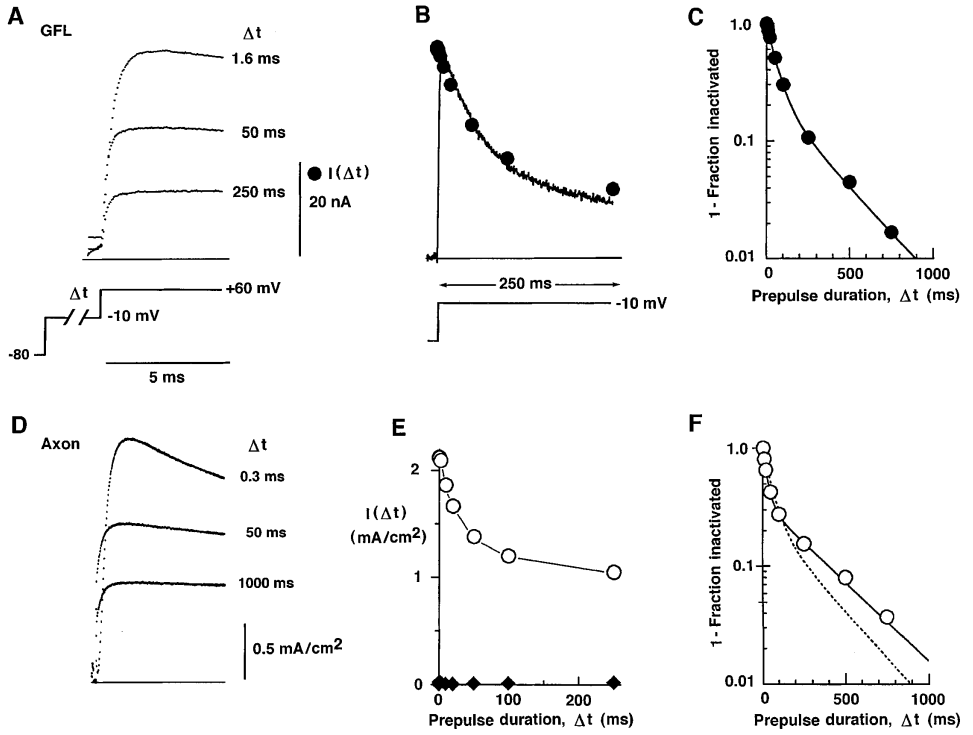

FIGURE 3. Fast and slow inactivation of delayed rectifier g_K. (*A*) Examples of I_K (Δt) at +60 mV after inactivating prepulses of increasing duration (Δt) to −10 mV in a GFL cell body. (18°C, 70 K_o//150 K_i.) (*B*) Kinetics of inactivation in a GFL neuron determined by two methods. I(Δt) values from the experiment described in A (●) are compared with the I_K waveform directly recorded at −10 mV. The I_K trace was scaled (×6.75) so that peak I_K = I (1.6 ms). (*C*) Inactivation kinetics in GFL neurons are not first-order. An inactivation index analogous to the *h* parameter (fraction not inactivated; Hodgkin and Huxley, 1952*b*) was computed for I(Δt) values (1.6–1,000 ms) from the experiment in *A* as:

$$1 - \textit{Fraction inactivated} = [I(\Delta t) - I_{1000}] / [I_{1.6} - I_{1000}],$$

where $I_{1.6}$ = I (1.6 ms) and I_{1000} represents the steady-state I(Δt) estimated with a 1,000-ms prepulse. The solid curve represents the best fit of the simplex algorithm (Sigma Plot 4.0; Jandel Scientific, Corte Madera, CA) to the equation:

$$1 - \textit{Fraction inactivated} = A_F \exp(-t/\tau_F) + A_s \exp(-t/\tau_S),$$

where $A_F + A_S = 1$. (*D*) I_K records at +60 mV obtained in a giant axon using the procedure described above (*A*) with prepulses of indicated durations to the estimated V_K of −7 mV. (18°C, 50 K_o//50 K_i.) (*E*) Time course of axonal g_K inactivation (○) determined by the prepulse method from the experiment in *D*. Filled diamonds represent values of I_K at the end of the prepulse (see text for additional details). (*F*) Bi-exponential inactivation kinetics similar to those in GFL neurons exist in giant axons. Data from panel *E* were analyzed as described above, and the bi-exponential fit is indicated by the solid curve. The time course of inactivation in the GFL neuron from panel *C* is given by the dashed line.

TABLE I

Comparison of Inactivation Properties in GFL Neurons and Giant Axons

	Fraction	Time Constants		Fractional Amplitudes	
	Inactivated	τ_F	τ_S	A_F	A_S
GFL	0.68 ± 0.03	52 ± 2.6 ms	289 ± 17 ms	0.77 ± 0.04	0.25 ± 0.03
	(n = 11)	(n = 11)	(n = 11)	(n = 11)	(n = 11)
Axon	0.41 ± 0.05	45 ± 7 ms	411 ± 72 ms	0.62 ± 0.04	0.39 ± 0.04
	(n = 3)	(n = 4)	(n = 4)	(n = 4)	(n = 4)

Population analysis (mean ± SEM; n = number of determinations) of results from GFL neurons and giant axons studied under similar conditions as described in the text. The fraction of g_K inactivated by 250-ms prepulses to voltages between −10 and 0 mV was calculated as 1- [I(250 ms)/I (1.6 ms)] as in Fig. 3. Fast (τ_F) and slow (τ_S) time constants and the respective fractional amplitudes (A_F and A_S) were determined with bi-exponential fits as described in the legend to Fig. 3. Although τ_F is comparable in GFL cells and giant axons, A_F is significantly larger in GFL cells ($P < 0.05$ by t test). GFL data were pooled from 9 different squid; axon data are from 2 different squid. GFL: 18°C, 70K_o//150 K_i. Axon: 18°C, 50 (or 70) K_o// 50 (or 70) K_i.

though significant inactivation exists in both cases, the total fraction of I_K inactivated within 250 ms in giant axons is smaller than that in cell bodies ($P < 0.05$ by t test). Values for fast (τ_F) and slow (τ_S) time constants are comparable in cell bodies and axons, and the fast component accounts for the majority of inactivating I_K in both cases.

Voltage Dependence of Inactivation Kinetics

Although measurements on giant axons are complicated by the requirement that inactivation can be studied only at voltages equal to V_K, experiments on GFL neurons are not thus limited. Prepulses to negative (−25 mV) or positive (+40 mV) voltages yield very different overall rates of inactivation, with either the slow or fast component predominating (Fig. 4 *A*). At −5 mV, a more even balance of fast and slow components exists. Bi-exponential fits to such data from a number of cells indicate that values of τ_F and τ_S are essentially voltage independent (Fig. 4 *B*), whereas the fractional amplitude of each component depends strongly on voltage. Fig. 4 *C* shows that the amplitude of the fast component (○ = A_F) increases as voltage becomes more positive, and the steep voltage dependence of A_F bears strong similarity to that of g_K measured in the same cell (◆). A_s decreases over the same voltage range, because $A_F + A_s = 1$.

Correspondence between the voltage dependencies of A_F and g_K suggests that the process underlying fast inactivation is strongly coupled to channel opening.

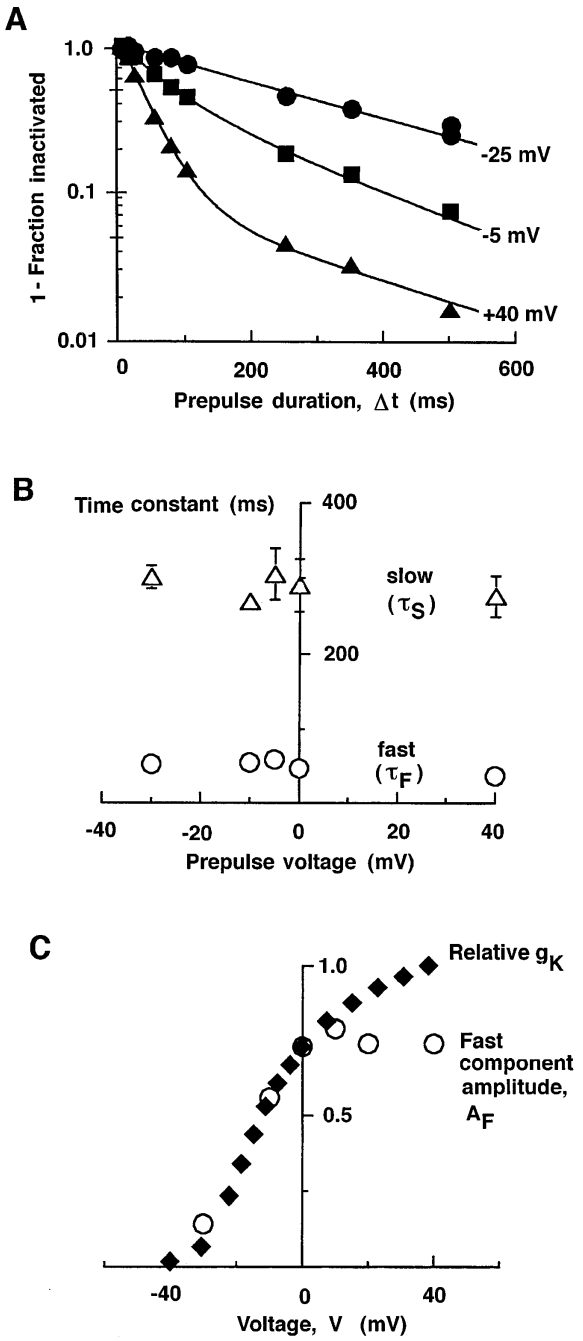

FIGURE 4. Voltage dependence of fast and slow components of inactivation in GFL neurons determined with the prepulse method. (*A*) Inactivation kinetics of g_K are illustrated for the indicated prepulse voltages. Inactivation proceeds faster at more positive voltages, and solid curves are bi-exponential fits as follows (values for τ in ms). At −25 mV: A_F = 0.05, τ_F = 100, A_S = 0.98, τ_S =361. At −5 mV: A_F = 0.53, τ_F = 67, A_S = 0.49, τ_S = 255. At +40 mV: A_F =0.96, τ_F = 39, A_S =0.10, τ_S = 307. (18°C, 20 K_o/150 K_i.) (*B*) Population analysis of the fast and slow time constants for inactivation derived from bi-exponential fits of data like those in panel *A*. Mean (±SEM) time constants for the fast (τ_F, ○) and slow (τ_S, △) components show little voltage dependence. n = 12 (+ 40 mV), 5 (0 mV), 3 (−10 mV), 3 (−30 mV). Conditions as in *A*. (*C*) Voltage dependence of the amplitude of the fast component of inactivation (A_F) determined in bi-exponential fits of data from a GFL cell (○). The voltage-dependence of g_K (◆) is very similar to that of A_F in the same cell. Relative g_K was measured as described in legend to Fig. 1 *D*. (18°C, 20 K_o//150 K_i.)

Conversely, predominance of the slow phase at negative voltages where g_K is small suggests that inactivation may also occur from closed states independently of channel opening or through a less directly coupled pathway.

Selective Modulation of Fast Inactivation

Fast inactivation in GFL neurons and axons can be reduced by withdrawal of internal MgATP. Consequences of omitting ATP from the pipette solution in whole-cell recordings from GFL neurons are illustrated in Fig. 5. After achieving the whole-cell configuration at time 0, a slow decline in both peak I_K (Fig. 5 *A*, *filled symbols*) and in the fraction of I_K inactivated during a 250 ms pulse to +40 mV (Fig. 5 *B*, *filled symbols*) typically occurs over 10–15 min. However, with 4 mM MgATP included in the pipette solution, both parameters are much more stable (*open symbols* in Fig. 5, *A* and *B*). Representative I_K traces taken at time 0 and after whole-cell dialysis are shown in Fig. 5, *C* (0 ATP) and *D* (4 mM ATP). At this voltage, most inactivation occurring on this time scale occurs via the fast pathway (Fig. 4 *C*). Although the pulses used for Fig. 5, *C* and *D*, were too short to allow reliable fitting of two exponentials to the falling phase of I_K, fitting single exponentials in Fig. 5 *C* yields time constants of 90 ms at time 0 and 200 ms at 620 s, consistent with a selective decrease in the fast component. A time constant of 85 ms adequately describes both traces in Fig. 5 *D*. Similar results were obtained for the other cells included in Fig. 5, *A* and *B*.

ATP was also necessary to maintain fast inactivation in perfused axons. The time course of inactivation with ATP in the internal perfusate is indicated in Fig. 6 (●), and ATP withdrawal for 30 min produced a decrease in both peak I_K and the amount of fast inactivation (○), comparable to the situation in GFL cells as described above.

At the end of the experiment, internal ATP was replaced, but neither peak I_K nor the degree of inactivation showed significant recovery within 15 min (not illustrated). Papain (1 mg/ml) was then introduced into the axon for 90 s and then washed out. This treatment produced an immediate decrease in peak I_K of ~50% and eliminated the fast component of inactivation (× in Fig. 6). A second application of papain produced no additional effect (not illustrated). ATP withdrawal and papain treatment were carried out in this manner in only one axon, but measurements made on two other axons which were both ATP deprived and papain treated failed to reveal significant inactivation occurring over 500 ms (not illustrated).

Preferential Effect of Temperature on Fast Inactivation Kinetics

Inactivation in both GFL cell bodies and giant axons is highly temperature dependent. Fig. 7 *A* displays I_K

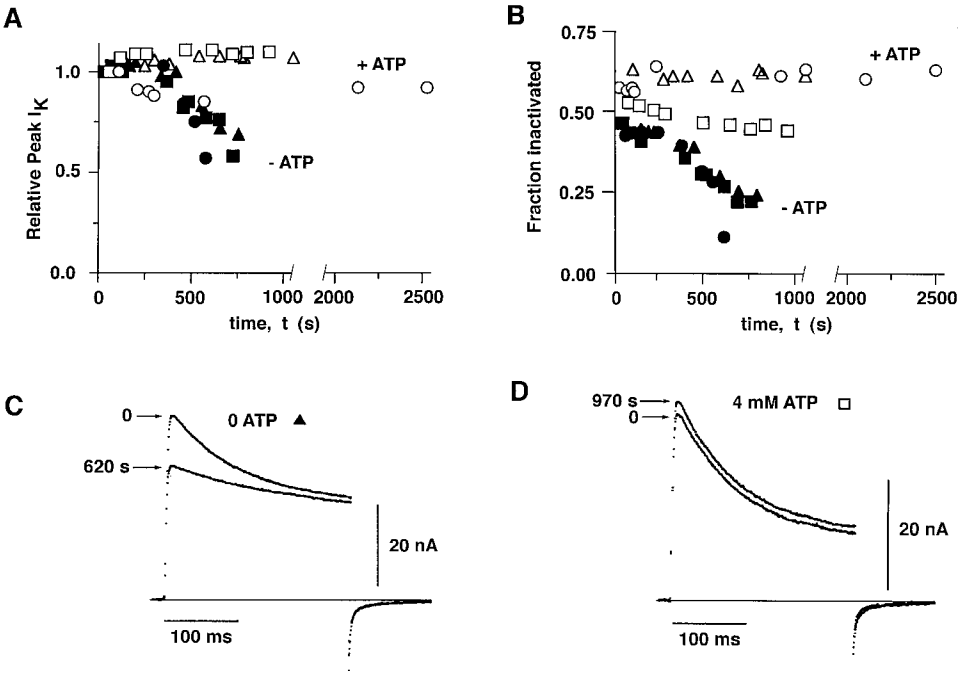

FIGURE 5. Omission of internal MgATP with GFL neurons reduces peak I_K and the amount of fast inactivation. (*A*) Peak I_K at each time point was measured at +40 mV and is plotted normalized to the first value (time 0) recorded after achieving the whole-cell configuration with (*open symbols*) and without (*filled symbols*) 4 mM MgATP in the pipette solution. Each symbol type represents a different cell. (10–12°C; 45 K_o//450 K_i [except □ = standard 20 K_o//150 K_i].) The composition of the 45 K_o external solution was (in mM): 45 KCl, 455 NaCl, 10 $MgCl_2$, 10 $CaCl_2$, 10 $MgSO_4$, 10 HEPES, and 0.0002 TTX at pH 7.66 (980 mosm). The 450 K_i internal solution contained (in mM): 60 KCl, 165 K glutamate, 165 K aspartate, 60 KF, 10 $MgSO_4$, 10.5 HEPES, 0.1 EGTA, 100 glycine, 21 tris base, 100 taurine and 100 betaine at pH 7.2 (~1,000 mosm). (*B*) Decline of the inactivating fraction of I_K during the same experiments as in panel *A*. The fraction of I_K inactivated was estimated directly from I_K recorded with 250-ms pulses to +40 mV as 1 − [I(250 ms) ÷ peak I_K]. (*C*) Elimination of ATP from the internal solution selectively decreases the rapidly inactivating portion of I_K (+40 mV) over a 10-min period after achieving the whole-cell configuration. Cell indicated by Δ in panels *A* and *B*. (*D*) Inclusion of 4 mM MgATP in the internal solution maintains fast inactivation. The I_K (+40 mV) trace of larger amplitude was recorded 17 min after the initial measurement. Cell indicated by □ in panels *A* and *B*.

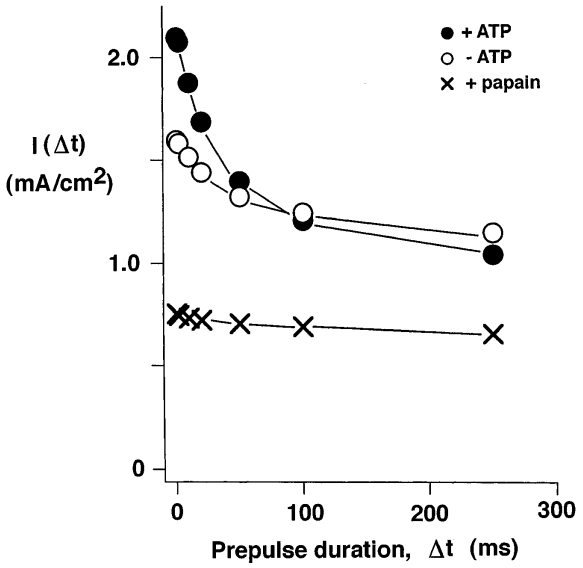

FIGURE 6. Reduction of inactivation in a giant axon produced by withdrawal of internal ATP and by papain treatment. Values of I(Δt) with the inactivating-prepulse procedure were determined with 4 mM MgATP in the internal perfusate (●), 30 min after removing ATP from the internal solution (○) and immediately after a 90-s treatment with internal papain (×). See text for additional details. Prepulses were to $V_K = -4$ to -7 mV as checked throughout the experiment. (18°C, 50 K_o//50 K_i.)

traces recorded at +60 mV from a GFL neuron at several temperatures between 5.5 and 26°C. Low temperature produces a decrease in peak I_K and a loss of fast inactivation similar to that seen with ATP withdrawal. Fig. 7 *B* shows inactivation kinetics at 12°C (○) and 18°C (●) determined with the prepulse method at 0 mV in a GFL cell. Solid curves are bi-exponential fits. The major effect of the temperature decrease is to reduce the rate of fast inactivation, with τ_F decreasing from 40 to 93 ms. The amplitude of the rapidly inactivating component is basically unchanged (A_F = 0.83 versus 0.76 at 18°C and 12°C, respectively), as is the slower time constant of inactivation (τ_S = 313 ms at 18°C and 265 ms at 12°C). Similar results were obtained in giant axons at these two temperatures (not illustrated).

Recordings made in a number (*n*) of GFL cells with prepulses to +40 mV yield mean values (± SEM) of τ_F = 82.4 ± 5.4 ms (*n* = 19) at 12°C and 37 ± 1.4 ms (*n* = 12) at 18°C. In these same experiments τ_S only changed from 365 ± 31 ms at 12°C to 282 ± 24 ms at 18°C. These figures correspond to Q_{10} values of 3.9 for τ_F and 1.5 for τ_S.

At temperatures below ~8°C, fast inactivation becomes undetectable. Fig. 7 *C* gives results from a prepulse-experiment at +40 mV in a GFL neuron at 18 and 8°C. Inactivation kinetics at 8°C (○) are adequately described by a single time constant (τ = 306 ms) comparable to that of the slow component at 18°C (●; τ_S = 295 ms, A_S = 0.21). In the same cell at −25 mV, a single time constant of 440 ms adequately described inactivation kinetics at both 18 and 8°C (not illustrated). These data reinforce the idea that the effect of temperature on inactivation kinetics is almost entirely due to changes in behavior of the fast component.

Effect of Temperature on "Steady-state" Inactivation

Temperature also exerts an effect on steady-state properties of inactivation. Fig. 8, *Ai* and *ii*, show I_K recorded at +40 mV following 1.5-s prepulses to the indicated voltages in a GFL neuron at 18 (●) and 8°C (○), respectively. Figure 8 *B* plots normalized peak I_K versus prepulse voltage from this experiment. Low temperature decreases the maximum fraction of steady-state inactivation and shifts the inactivation-voltage relation by about −15 mV but does not significantly change its shape, i.e., steepness.

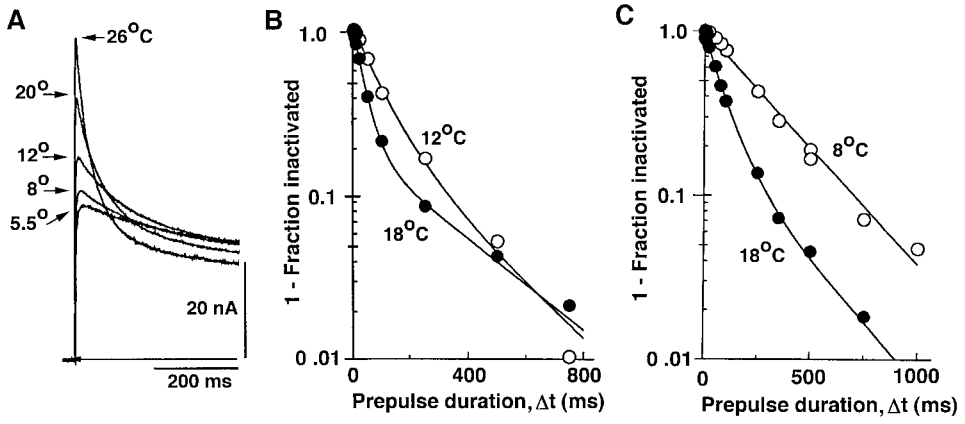

FIGURE 7. Temperature dependence of fast inactivation. (*A*) I_K at +60 mV in a GFL cell was recorded over a range of temperature as indicated. (20 K_o//150 K_i.) (*B*) Kinetic analysis and bi-exponential fits of inactivation for a GFL cell at 12 and 18°C. Prepulses were to 0 mV. See text for fit parameters. (20 K_o//150 K_i.) (*C*) Inactvation kinetics from another GFL cell with prepulses to +40 mV at 8 and 18°C. Inactivation kinetics are monoexponential at 8°C. Fit parameters at 18°C: τ_F = 86 ms, τ_S = 295 ms, A_F = 0.75, A_S = 0.21. Single time constant fit at 8°C has a value of 306 ms. (20 K_o//150 K_i.)

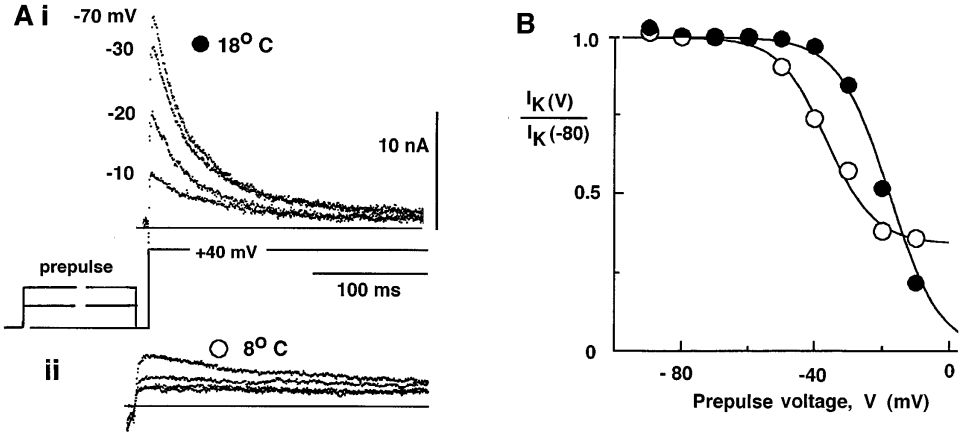

FIGURE 8. Temperature dependence of steady-state inactivation. (*Ai*) I_K at +40 mV after 1.5-s prepulses to the indicated values at 18°C. A 5-ms repolarization to −80 preceeded each test pulse. (*Aii*) Analogous records at 8°C in same cell. (*B*) Relationship between available I_K and prepulse voltage derived from the records in panels *Ai* (●; 18°C) and *Aii* (○; 8°C). Peak amplitude of each test I_K has been normalized to I_K recorded with a prepulse to −80 mV. Solid curves were drawn by eye. (20 K_o//150 K_i.)

Recovery from Inactivation in GFL Neurons and Giant Axons

Recovery from inactivation was studied in giant axons and GFL cells under similar conditions using a standard protocol. Fig. 9 *A* shows results from a GFL experiment at 18°C. The inactivating prepulse to +40 mV lasted 250 ms, and the amount of inactivation is indicated by the decrease of I_K from its peak value to the final value at the end of the prepulse (I_{SS}). Sampling was

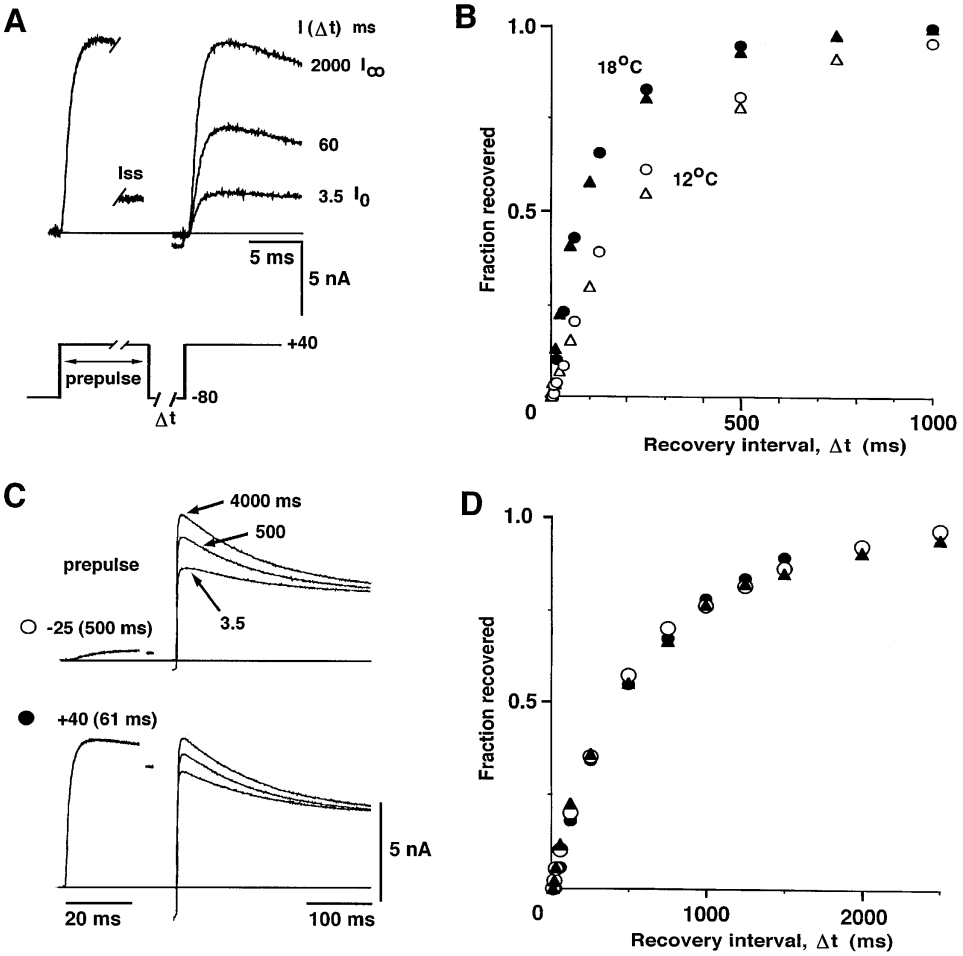

FIGURE 9. Recovery from inactivation in GFL neurons and giant axons. (*A*) Examples of I_K (tested at +40 mV) during recovery from inactivation produced by a 250-ms prepulse to +40 mV in a GFL cell body were made using the protocol diagrammed in the inset. Values of Δt correspond to the recovery period at −80 mV; examples for 2,000 ms (I_∞ = nearly full recovery), 60 and 3.5 ms (I_0 = no recovery) are shown. The extent of inactivation produced by the first pulse is given by the difference between peak I_K and I_K measured at the end of the pulse (I_{ss}). (18°C, 70 K_o//150 K_i.) (*B*) Recovery kinetics in GFL cell bodies and giant axons are similar. The time course of fractional I_K recovery was computed for I(Δt) values (3.5–1,000 ms) as described in the text. Values for the GFL cell of panel A are plotted at 18 (●) and 12°C (○). Triangles illustrate data obtained in a giant axon using inactivating prepulses of 500-ms duration to −7 mV at 18°C (▲) and 12°C (△). (18°C, 50 K_o//50 K_i.) (*C*) Different prepulse procedures were used to inactivate g_K in a GFL neuron slowly (○, 500-ms prepulse to −25 mV—upper set of traces) and primarily by the fast pathway (●, 61-ms prepulse to +40 mV—lower set of traces). Records for Δt values of 3.5 ms (I_0), 500 ms, and 4,000 ms (I_∞) are shown for each protocol. (*D*) Recovery kinetics are comparable regardless of whether g_K inactivates by the fast or slow pathway. Recovery at −80 mV was measured for the GFL cell of panel *C* using both prepulse protocols (symbols as in *C*) and analyzed as described above. Measurements were also made using a 500-ms prepulse to 0 mV (▲). (12°C, 20 K_o//150 K_i.)

turned off during most of the prepulse and also for most of the recovery period, Δt. The increase of I(Δt) above I_{SS} represents recovery after a time (Δt) at −80 mV, and the fraction of I_K recovered was computed as $[I(\Delta t) - I_0]/[I_\infty - I_0]$, where I_0 = I (3.5 ms) (no recovery) and I_∞ = I (2,000 ms) (nearly complete recovery). The time course of recovery thus defined is shown in Fig. 9 *B* (●). A similar recovery time course was obtained in a giant axon with an inactivating prepulse to V_K = −7 mV (▲). Open symbols in Fig. 9 *B* give results from the same GFL neuron (○) and axon (△) at 12°C. In no case does recovery follow an exponential time course.

Because inactivation can proceed by fast and slow pathways, recovery kinetics in GFL cells were compared for inactivating pulses that primarily produced either fast or slow inactivation. In order to preferentially inactivate channels slowly, a prepulse was made to −25 mV for 500 ms (Fig. 9 *C, upper records*). Nearly pure fast inactivation was obtained with a prepulse to +40 mV for 61 ms (Fig. 9 *C, lower records*). If inactivation produced by these pulse protocols put channels into distinct inactivated states, recovery kinetics might be different in the two cases. This expectation was not born out, however. Results in Fig. 9 *D* indicate that the slow (○) and fast (●) inactivation protocols yielded the same recovery time course, as did a prepulse to 0 mV for 500 ms which produced mixed slow and fast inactivation (▲).

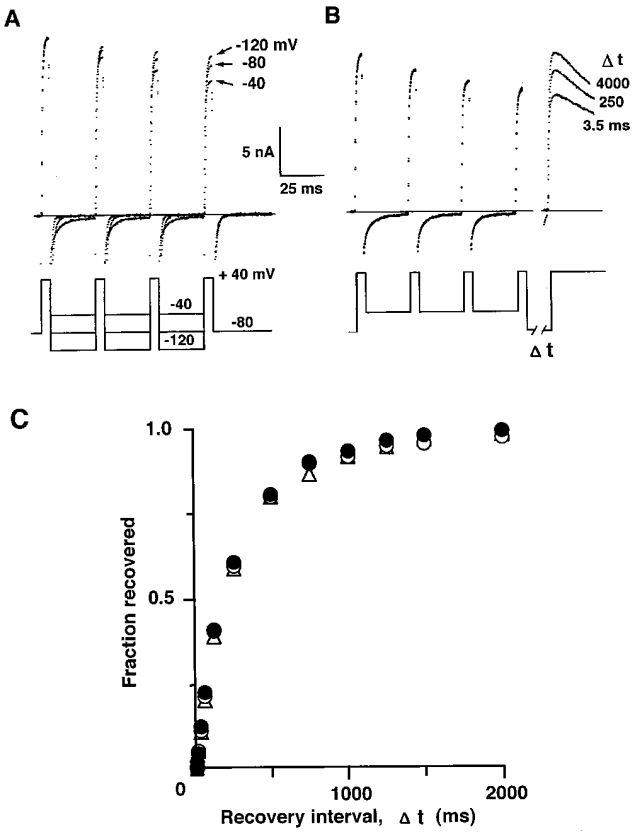

FIGURE 10. Cumulative inactivation of I_K in GFL neurons. (*A*) Repetitive pulsing (5 ms to +40 mV) every 30 ms produces an accumulating decrease of I_K. Three continuous records are illustrated for different inter-pulse voltages. (18°C, 20 K_o//150 K_i.) (*B*) Recovery of I_K following four repetitive pulses as in A (inter-pulse voltage of −40 mV). Three superimposed traces correspond to the indicated recovery intervals (Δt) at −80 mV. Same cell as in *A*. (*C*) Recovery from cumulative inactivation (△) proceeds with the same time course as recovery from ordinary fast inactivation (○) produced by a strong, brief pulse (+40 mV for 36 ms) or from mixed fast and slow inactivation (●) produced by a long pulse (+40 mV for 250 ms). Recovery kinetics were analyzed as described in conjunction with Fig. 10.

Cumulative Inactivation

Application of brief, repetitive pulses produces an accumulating decrease in the amplitude of I_K in GFL neurons, and this decrease is more prominent if the inter-pulse voltage is made more positive. Fig. 10 *A* illustrates these effects for 5-ms pulses applied every 30 ms with inter-pulse voltages of −40, −80, and −120 mV. These results are characteristic of cumulative inactivation (Aldrich et al., 1979). Development of cumulative inactivation continues as long as channels are open, including the time when tail currents are flowing, and the largest decrease of I_K thus occurs with an inter-pulse voltage of −40 mV where channel closing is slow. Although cumulative inactivation is generally associated with C-type inactivation in mammalian (Lee and Deutsch, 1990; Marom and Levitan, 1994) and *Shaker* (Baukrowitz and Yellen, 1995) Kv1 channels, it is not clear at this stage if this phenomenon occurs only with C-type mechanisms.

Very little "ordinary" fast (or slow) inactivation of squid g_K occurs in 5 ms, so repetitive pulsing provides a third way to selectively inactivate channels. Recovery from the cumulative-inactivated condition was therefore studied to shed light on the relationship of this inactivation pathway to the fast and slow processes. Fig. 10 *B* shows recovery at −80 mV from the effect of four brief pulses for recovery periods of (Δ t) = 3.5 ms (no recovery), 250 ms, and 4,000 ms (full recovery). Analysis of recovery kinetics in this experiment is presented in Fig. 10 *C*. Recovery from cumulative inactivation (Δ) proceeds with the same time course as recovery from fast inactivation (○) or from mixed fast and slow inactivation (●) produced as described above. These results indicate that the cumulative-inactivated state is not readily distinguishable from the inactivated state (or states) reached via fast or slow inactivation.

Two observations suggest that cumulative inactivation in squid K channels may be associated with processes underlying fast inactivation. First, the amount of cumulative inactivation induced by a single 5–10-ms pulse is greater at 18°C (19 ± 2%, n = 5) than at 12°C (11 ± 2%, n = 14). This temperature-sensitivity (Q_{10} = 2.5) is less than that shown by the rate of fast inactiva-

tion (Q_{10} = 3.7; 38 ± 2 ms at 18°C versus 82 ± 7 ms at 12°C, determined in the same cells by bi-exponential fitting), but it is considerably greater than that of the slow rate of inactivation (Q_{10} = 1.5). Second, a fair correlation exists between the degree of cumulative inactivation and the fraction of I_K inactivated during a 250-ms pulse at 12 or 18°C (data not illustrated).

Dependence of Inactivation on External Potassium

External potassium ions are known to exert a strong influence on the kinetics of C-type inactivation of Kv1 channels, including *Shaker* B (Lopez-Barneo et al., 1993; Baukrowitz and Yellen, 1995) and mammalian Kv1.3 (Marom and Levitan, 1994; Levy and Deutsch, 1996) and Kv1.4 (Pardo et al., 1992; Rasmusson et al., 1995). In light of the results on cumulative inactivation, which suggest some similarity between C-type inactivation and the fast process in squid K channels, experiments were carried out on GFL neurons in which the effects of elevated external K on inactivation were assessed.

Fig. 11 *A* shows I_K traces recorded at +60 mV in the presence of 5–500 mM external K. Although the amount of inactivation clearly depends on external K, very little effect of high K on inactivation kinetics is evident. This impression is supported by the kinetic analysis of prepulse-procedure data obtained in 5 mM (○) and 200 mM (●) external K (Fig. 11 *B*). Fig. 11 *C* presents the steady-state relation between inactivation and voltage measured with 1.5-s prepulses in 5 mM (○) and 200 mM (●) K. High K primarily decreases the maximum degree of inactivation.

Recovery from inactivation in GFL neurons is accelerated in high external K. Fig. 11 *D* shows the recovery time course in the presence of 5 mM (○) and 200 mM (●) external K. The time course in high K remains nonexponential. Accelerated recovery from inactivation in high external K occurs with both C- and N-type mechanisms in Kv1 channels (Demo and Yellen, 1991; Gomez-Lagunas and Armstrong, 1994; Rasmusson et al., 1995; Levy and Deutsch, 1996).

Effect of External TEA on Inactivation

Competition with internal and external TEA is known to slow the rates of N- and C-type inactivation, respectively (Choi et al., 1991), and sensitivity to external TEA has been used as a diagnostic feature to identify C-type inactivation (Rasmusson, et al., 1995). Although results in Fig. 2 show that neither external nor internal TEA markedly alter inactivation kinetics of squid delayed rectifier g_K, the effects of external TEA were examined more carefully. Fig. 12 *Ai* shows the reduction in I_K at +40 mV (○) by 500 mM external TEA (●). To facili-

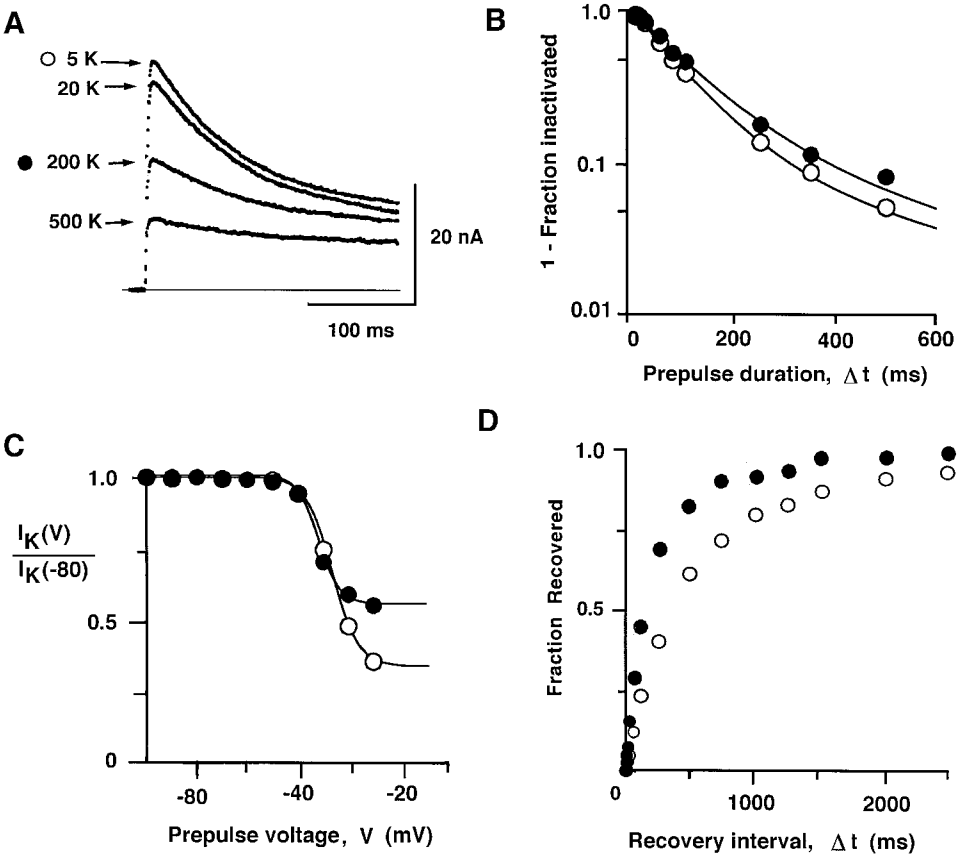

FIGURE 11. Inactivation in GFL neurons is sensitive to external K. (*A*) I_K at +40 mV recorded in a GFL cell body at the indicated external K concentrations. The major effect of high K is a decrease in the fraction of I_K inactivated. (12°C, 5–500 K_o//150 K_i.) (*B*) Inactivation kinetics, determined by the prepulse method for the same cell as in panel *A*, are similar in 200 mM (●) versus 5 mM (○) K. Bi-exponential fit parameters for 5 mM K_o are τ_F = 98 ms, τ_S= 498 ms, A_F = 0.90, A_S = 0.12. Parameters for 200 K_o are τ_F = 111 ms, τ_S= 435 ms, A_F = 0.84, A_S = 0.19. (*C*) Relationship between steady-state inactivation and voltage (see text and legend to Fig. 9) was determined in 200 mM (●) and 5 mM (○) external K. The only major difference lies in the maximum fraction inactivated. Smooth curves were drawn by eye. Same cell as in *A*. (*D*) Recovery from inactivation occurs more quickly in 200 mM (●) than in 5 mM (○) external K. Recovery kinetics following a long pulse (250 ms to +40 mV were analyzed as described above. Same cell as in *A*.

tate comparison of inactivation kinetics, the traces are replotted in Fig. 12 *Aii* after fitting the baseline to the I_K level at the end of the pulse along with a version of the record in TEA (*arrow*) scaled to the control peak I_K. Although the control and scaled TEA traces show a similar early time course, they deviate at later times, with the TEA trace decaying more slowly. These traces are plotted with superimposed bi-exponential fits in Fig. 12 *Aiii* (see legend). Neither the fast nor slow time constant appears to be increased by TEA, and the major effect of external TEA is a decrease in A_F. This result is quite different from that seen in studies of cloned Kv1 channels.

Results of the prepulse method for determining inactivation kinetics in the same cell are shown in Fig. 12 *B*. Although the effect at +20 mV (○, control; ●, TEA) is similar to that described above, there is no comparable effect at −30 mV (△, control; ▲, TEA), consistent with the fact that little inactivation occurs by the fast pathway at such negative voltages. Although the slowing of inactivation by external TEA in this manner is subtle, this effect was seen in each of four cells studied in the presence of TEA at concentrations sufficient to block I_K by ≥50%.

Internal TEA does not appear to alter the kinetics of inactivation at either 12 or 18°C. I_K at +40 mV was periodically monitored with 250–500-ms pulses during the initial period of intracellular dialysis with the standard internal solution plus 1.6 mM TEA-Cl as described in conjunction with Fig. 2, *E* and *F*. Although this procedure regularly led to a decrease in peak I_K of ≥50% over 5–10 min, there was no consistent effect of the kinetics of the decaying portion of I_K when traces were compared as described for Fig. 12 *A* (not illustrated).

DISCUSSION

This paper describes inactivation properties of delayed rectifier g_K in squid giant axons and in the cell bodies of GFL neurons from which these axons arise. Inactivation of g_K shows similar complex properties in both parts of this system and proceeds with two kinetic components, the faster of which has a time constant of ~50 ms at 18°C. The fast component is very sensitive to temperature, becoming undetectable below 8°C, and requires internal ATP. The slower component (time constant of ~300 ms) is not much affected by either temperature or ATP.

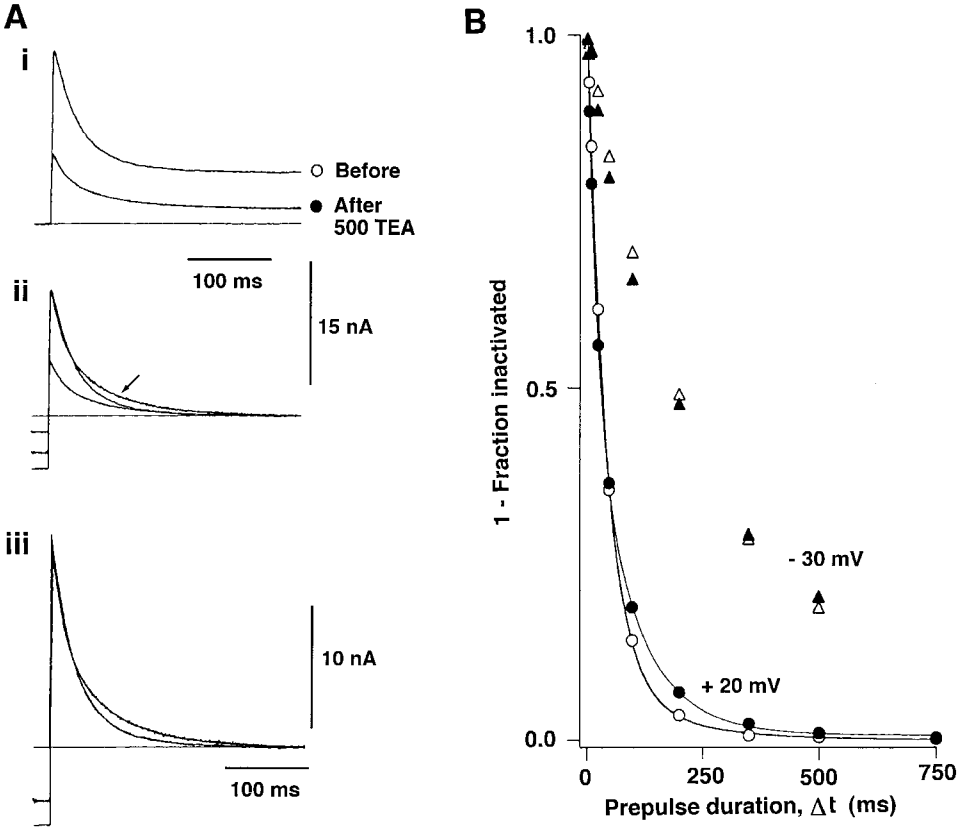

FIGURE 12. Effect of external TEA on inactivation kinetics in GFL neurons. (*Ai*) I_K at +40 mV is plotted before (○) and after (●) replacing 500 mM external Na with TEA. (*Aii*) Traces in (*i*) are plotted after fitting baselines to I_K at 500 ms; the TEA trace is also plotted after scaling (×2.3; *arrow*) to match control peak I_K. (*Aiii*) Control and scaled TEA traces of (*ii*) are superimposed with double exponential fits. Control: τ_F = 38 ms, A_F = 0.88, τ_S = 130 ms, A_S = 0.12. TEA: τ_F = 25 ms, A_F = 0.52, τ_S = 100 ms, A_S = 0.48. (18°C, 5 K_o//150 K_i.) The standard external solution was modified to contain 500 mM NaCl, 5 KCl, 5 $CaCl_2$, 20 $MgCl_2$; other constituents were unchanged. In the 500 mM TEA external solution, TEA-Cl replaced NaCl, but 60 mM NaCl was added to maintain proper osmolality. (*B*) Inactivation time course determined with the prepulse method at +20 mV (*circles*) and −30 mV (*triangles*) in the absence (*open symbols*) and presence (*filled symbols*) of 500 mM TEA. Solid curves are bi-exponential fits to the data at +20 mV. Control: τ_F = 40 ms, A_F = 0.92, τ_S = 150 ms, A_S = 0.08. TEA: τ_F = 22 ms, A_F = 0.49, τ_S = 95 ms, A_S = 0.54. Same cell and conditions as in *A*.

Similarities between fast inactivation in GFL neuron cell bodies and giant axons as described in this paper are consistent with the conjecture that the relevant K channels are encoded by the same mRNA, SqKv1A (Rosenthal et al., 1996). We have not yet carried out detailed studies of inactivation in the cloned channel, however. The present work provides a more complete picture of inactivation of the native channels which will guide analysis of SqKv1A.

Complex Inactivation of Squid Delayed Rectifier g_K

Fast and slow inactivation processes of squid K channels interact in important and seemingly novel ways. Although the rates of fast and slow inactivation individually show little voltage dependence, the overall time course of inactivation is quite voltage dependent. This comes about by a shift in the balance between the fraction of channels inactivating by the complementary pathways. Growth of the fast-inactivating fraction with voltage matches the voltage dependence of g_K, suggesting that the fast-inactivating pathway is very accessible from the open state. At voltages negative to −25 mV, the probability of channel opening is relatively low, and most channels that inactivate in this voltage range do so slowly.

Steady-state inactivation is fairly prominent over this voltage range, however, suggesting that the slow inactivation processes may also be important in determining steady-state properties. Low temperature (8 vs. 18°C) does not significantly alter the g_K-V relation (not illustrated), but it does shift the voltage dependence of steady-state inactivation. This would be consistent with the idea that slow inactivation can occur from closed states in the activation pathway, the kinetics of which are quite temperature sensitive.

Recovery from inactivation shows a nonexponential time course, but there are not two kinetic components corresponding to the fast and slow inactivation processes. Regardless of whether inactivation occurs via the fast or slow pathway, or by a cumulative-type process, recovery proceeds with the same time course. Multiple inactivation pathways thus appear to either converge on a single inactivated state or lead to a pool of inactivated states that are likely to be in rapid equilibrium at voltages where recovery is measured.

Inactivation of the squid delayed rectifier appears to be unusually complex, and it is very likely that this complexity is responsible for variability in the amount of fast inactivation seen between different cells and between cell bodies and axons. At present a specific kinetic scheme for inactivation cannot be uniquely identified. In any such model the rates and amounts of inactivation from closed versus open states depend not only on the rates of the inactivation steps themselves but also on details of the activation pathway leading into and out of the open state (Hoshi et al., 1994; Zagotta et al., 1994*a*, *b*). Such data are not yet available for squid channels.

Reduction of Fast Inactivation by Withdrawal of Internal ATP

Functional modification of squid axon K channels by internal ATP has been extensively studied at the macroscopic (Perozo et al., 1989; Augustine and Bezanilla, 1990) and single channel (Perozo et al., 1991) levels. All effects of the putative phosphorylation event were accounted for by a shift of activation and steady-state inactivation properties along the voltage axis by ∼+20 mV (Perozo and Bezanilla, 1990, 1991).

In this paper we show that internal ATP is necessary to maintain fast inactivation in both axons and cell bodies. ATP withdrawal produces a decrease in peak I_K and a reduction in the amount of fast inactivation. Both of these effects appear to be independent of the effects on voltage-dependent properties expected to accompany ATP withdrawal (i.e., a 20-mV hyperpolarizing shift), because our experiments were carried out with very negative holding potential (−80 mV) and positive test potentials (+40 mV or higher).

Presumably, the fast inactivation mechanism is operative only in the phosphorylated condition, but we have no direct evidence for this. The site(s) of phosphorylation need not be the same as those responsible for effects on voltage-dependent gating, and it is likely that reported effects of phosphorylation on steady-state inactivation indirectly reflect the effects on activation gating (Perozo and Bezanilla, 1991). A role for phosphorylation in determining the rate of C-type inactivation in mammalian Kv1.3 channels has been proposed, but the precise nature of this regulation remains to be determined (Kupper et al., 1995).

Is Fast Inactivation in Squid N-type or C-type?

Delayed rectifier K channels in squid are quite sensitive to internal TEA, but slowing of inactivation was not observed in the presence of internal TEA. This suggests that neither fast nor slow inactivation in is mediated by an N-type mechanism involving intracellular pore-block (Choi et al., 1991). Although elimination of fast inactivation by internal papain (Fig. 6) might suggest an intracellular, N-type mechanism, we do not regard irreversible protease sensitivity as definitive.

Dependence of inactivation kinetics on external K and TEA, along with the presence of significant cumulative inactivation are associated with C-type inactivation mechanisms that involve the extracellular mouth of the channel (Liu et al., 1996). Several features of fast inactivation of squid g_K are to some extent similar to results obtained in cloned channels showing C-type inactivation, but some clear differences deserve comment.

In the case of external TEA and high K, the time course of inactivation in squid is not altered very much, and the primary effect we describe is a selective decrease in the amount of fast inactivation. These results are clearly not equivalent to those in other systems where the actual rate of inactivation is slowed (Lopez-Barneo et al., 1993; Marom and Levitan, 1994; Baukrowitz and Yellen, 1995; Rasmusson et al., 1995; Levy and Deutsch, 1996).

On the other hand, changes in the amount of inactivation produced by these modifiers of C-type processes may not be unique to squid K channels. C-type inactivation in *Shaker* (Oglieska et al., 1995) and mammalian (Panyi et al., 1995; Rasmusson et al., 1995) Kv1 channels is incomplete, even in low external K, and a decrease in the amount of inactivation in high external K appears to accompany the decreased inactivation rate (Lopez-Barneo et al., 1993; Marom and Levitan, 1994; Baukrowitz and Yellen, 1995).

We have proposed elsewhere that the delayed rectifier g_K in GFL neurons and giant axons corresponds to protein encoded by the cDNA SqKv1A (Rosenthal et al., 1996). The predicted NH_2 terminus of this protein shows little similarity to features known to be important to N-type inactivation in *Shaker* variants (Hoshi et al., 1990; Murrel-Lagnado and Aldrich, 1993). Structural determinants of N-type inactivation in rat Kv1.4 (Tseng-Crank et al., 1993) are not identical to those in *Shaker*, however, and some form of N-type inactivation for the SqKv1A α subunit cannot be ruled out based on sequence data alone.

Presently there is no molecular structure that defines C-type inactivation, but specific residues in *Shaker* B (e.g., T449) are critically important to the rate of inactivation and its dependence on external K (Lopez-Barneo et al., 1993; Baukrowitz and Yellen, 1995). SqKv1A has a serine at the position equivalent to *Shaker* T449 (Rosenthal et al., 1996), and the T449S mutation in *Shaker* produces extremely fast C-type inactivation (Schlief et al., 1996).

Although a plausible case can be made for fast inactivation of squid K channels being related to a C-type process, the relationship would appear to be rather distant. It is even less clear how the slower process in squid fits in. The lack of a simple correspondence between N- or C-type processes may not, in fact, be that surprising, since both processes have been carefully studied in only a few channel types (mainly *Shaker*), and their properties depend not only on the inactivation mechanisms themselves, but on the molecular and kinetic coupling to other aspects of channel function (Baukrowitz and Yellen, 1995). Future work on the cloned squid delayed rectifier in heterologous expression systems will reveal how inactivation compares to that described here for the native channels in giant axons and GFL neurons.

This work was supported by grants from the National Institutes of Health (NS-12547 to C.M. Armstrong and NS-17510 to W.F. Gilly) and by an ONR AASERT award to J.J.C. Rosenthal.

Original version received 25 October 1996 and accepted version received 9 January 1997.

REFERENCES

Aldrich, R.W., Jr., P.A. Getting, and S.H. Thompson. 1979. Inactivation of delayed outward current in molluscan somata. *J. Physiol. (Lond.).* 291:507–530.

Armstrong, C.M., and W.F. Gilly. 1992. Access resistance and space clamp problems associated with whole-cell patch clamping. *Methods Enzymol.* 207:100–122.

Augustine, C.K., and F. Bezanilla. 1990. Phosphorylation modulates potassium conductance and gating current of perfused giant axons of squid. *J. Gen. Physiol.* 95:245–271.

Baukrowitz, T., and G. Yellen. 1995. Modulation of K^+ current by frequency and external $[K^+]$: a tale of two inactivation mechanisms. *Neuron.* 15:951–960.

Chabala, L.D. 1984. The kinetics of recovery and development of potassium channel inactivation in perfused squid (*Loligo pealei*) giant axons. *J. Physiol. (Lond.).* 356:193–220.

Choi, L.L., R.W. Aldrich, and G. Yellen. 1991. Tetraethylammonium blockade distinguishes two inactivation mechanisms in voltage-activated K channels. *Proc. Natl. Acad. Sci. USA.* 88:5092–5095.

Clay, J.R. 1989. Slow inactivation and reactivation of the K^+ channel in squid axons. A tail current analysis. *Biophys. J.* 55:407–414.

Demo, S.D., and G. Yellen. 1991. The inactivation gate of the Shaker K channel behaves like an open-channel blocker. *Neuron.* 7:743–753.

Ehrenstein, G., and D.L. Gilbert. 1966. Slow changes of potassium permeability in the squid giant axon. *Biophys. J.* 6:553–566.

Frankenhaeuser, B., and A.L. Hodgkin. 1956. The after-effects of impulses in the giant nerve fibres of *Loligo. J. Physiol. (Lond.).* 131: 341–376.

Gilly, W.F., and C.M. Armstrong. 1982. Slowing of sodium channel opening kinetics in squid axon by extracellular zinc. *J. Gen. Physiol.* 79:935–964.

Gilly, W.F., M.T. Lucero, and F.T. Horrigan. 1990. Control of the spatial distribution of sodium channels in giant fiber lobe neurons of the squid. *Neuron.* 5:663–674.

Gomez-Lagunas, F., and C.M. Armstrong. 1994. The relation between ion permeation and recovery from inactivation of *Shaker* B K^+ channels. *Biophys. J.* 67:1806–1815.

Hodgkin, A.L., and A.F. Huxley. 1952*a*. Currents carried by sodium and potassium ions through the membrane of the giant axon of *Loligo. J. Physiol. (Lond.).* 116:449–472.

Hodgkin, A.L., and A.F. Huxley. 1952*b*. A quantitative description of membrane current and its application to conduction and excitation in nerve. *J. Physiol. (Lond.).* 117:500–544.

Horrigan, F.T., and W.F. Gilly. 1996. Methadone block of K^+ currents in squid giant fiber lobe neurons. *J. Gen. Physiol.* 107:243–260.

Hoshi, T., W.N. Zagotta, and R.W. Aldrich. 1990. Biophysical and molecular mechanisms of *Shaker* potassium channel inactivation. *Science (Wash. DC).* 250:533–538.

Hoshi, T., W.N. Zagotta, and R.W. Aldrich. 1994. *Shaker* potassium

channel gating. I Transitions near the open state. *J. Gen. Physiol.* 103:249–278.

Jan, L.Y., and Y.N. Jan. 1992. Structural elements involved in specific K^+ channel functions. *Annu. Rev. Physiol.* 54:537–555.

Keynes, R.D. 1994. The kinetics of voltage-gated ion channels. *Q. Rev. Biophys.* 27:339–434.

Kupper, J., M.R. Bowlby, S. Marom, and I.B. Levitan. 1995. Intracellular and extracellular amino acids that influence C-type inactivation and its modulation in a voltage-dependent potassium channel. *Pflüg. Arch. Eur. J. Physiol.* 430:1–11.

Lee, C.S., and C. Deutsch. 1990. Temperature dependence of K^+-channel properties in human T lymphocytes. *Biophys. J.* 57:49–62.

Levy, D.I., and C. Deutsch. 1996. Recovery from C-type inactivation is modulated by extracellular potassium. *Biophys. J.* 70:798–805.

Liu, Y., M.E. Jurman, and G. Yellen. 1996. Dynamic rearrangement of the outer mouth of a K channel during gating. *Neuron.* 16: 859–867.

Llano, I., and R.J. Bookman. 1986. Ionic conductances of squid giant fiber lobe neurons. *J. Gen. Physiol.* 88:543–569.

Llano, I., C.N. Webb, and F. Bezanilla. 1988. Potassium conductance of the squid giant axon. Single channel studies. *J. Gen. Physiol.* 92:179–196.

Lopez-Barneo, J., T. Hoshi, S.H. Heinemann, and R.W. Aldrich. 1993. Effects of external cations and mutations in the pore region on C-type inactivation of *Shaker* potassium channels. *Receptors and Channels* 1:61–71.

Marom, S., and I.B. Levitan. 1994. State-dependent inactivation of the Kv3 potassium channel. *Biophys. J.* 67:579–589.

McFarlane, M.B., and W.F. Gilly. 1996. Spatial localization of calcium channels in giant fiber lobe neurons of the squid (*Loligo opalescens*). *Proc. Natl. Acad. Sci. USA.* 93:5067–5071.

Murrell-Lagnado, R.D., and R.W. Aldrich. 1993. Interactions of amino terminal domains of Shaker K channels with a pore blocking site studied with synthetic peptides. *J. Gen. Physiol.* 102:949–975.

Nealey, T., S. Spires, R.A. Eatock, and T. Begenisich. 1993. Potassium channels in squid neuron cell bodies: comparison to axonal channels. *J. Membr. Biol.* 132:13–25.

Oglieska, E.M., W.N. Zagotta, T. Hoshi, S.H. Heinemann, J. Haab, and R.W. Aldrich. 1995. Cooperative subunit interaction in C-type inactivation of K channels. *Biophys. J.* 69:2449–2457.

Panyi, G., Z. Sheng, L. Tu, and C. Deutsch. 1995. C-type inactivation of a voltage-gated K channel occurs by a cooperative mechanism. *Biophys. J.* 69:896–903.

Pardo, L.A., S.H. Heinemann, H. Terlau, U. Ludewig, C. Lorra, O. Pongs, and W. Stuhmer. 1992. Extracellular K^+ specifically modulates a rat brain K^+ channel. *Proc. Natl. Acad. Sci. USA.* 89:2466–2470.

Perozo, E., and F. Bezanilla. 1989. Modulation of K channels in dialyzed squid axons. ATP-mediated phosphorylation. *J. Gen. Physiol.* 93:1195–1218.

Perozo, E, and F. Bezanilla. 1990. Phosphorylation affects voltage gating of the delayed rectifier K^+ channel by electrostatic interactions. *Neuron.* 5:685–690.

Perozo, E., and F. Bezanilla. 1991. Phosphorylation of K^+ channels in the squid giant axon. A mechanistic analysis. *J. Bioenerget. Biomembr.* 23:599–613.

Perozo, E., D.S. Jong, and F. Bezanilla. 1991. Single channel studies of the phosphorylation of K^+ channels in the squid giant axon. II. Nonstationary conditions. *J. Gen. Physiol.* 98:19–34.

Pongs, O. 1992. Molecular biology of voltage-dependent potassium channels. *Physiol. Rev.* 72:S69–S88.

Rasmusson, R.L., M.J. Morales, R.C. Castellina, Y. Zhang, D.L. Campbell, and H.C. Strauss. 1995. C-type inactivation controls recovery in a fast-inactivating cardiac K channel (Kv1.4) expressed in *Xenopus* oocytes. *J. Physiol. (Lond.).* 489:709–721.

Rosenthal, J.J.C., R.G. Vickery, and W.F. Gilly. 1996. Molecular identification of SqKv1A: a candidate for the delayed rectifier K channel in squid giant axon. *J. Gen. Physiol.* 108:1–13.

Rudy, B. 1988. Diversity and ubiquity of K channels. *Neruoscience.* 25:729–749.

Schlief, T., R. Schonherr, and S.H. Heinemann. 1996. Modification of C-type inactivating Shaker potassium channels by chloramine-T. *Pflüg. Arch. Eur. J. Physiol.* 431:483–493.

Tseng-Crank, J., J.-A. Yao, M.F. Berman, and G.-N. Tseng. 1993. Functional role of the NH_2-terminal domain of a mammalian A-type K channel. *J. Gen. Physiol.* 102:1057–1083.

Werkman, T.R., T.A. Gustafson, R.S. Rogowski, M.P. Blaustein, and M.A. Rogawski. 1993. Tityustoxin-Kα, a structurally novel and highly potent K channel peptide toxin, interacts with the α-dendrotoxin binding site on the cloned Kv1.2 K channel. *Mol. Pharm.* 44:430–436.

Zagotta, W.N., T. Hoshi, and R.W. Aldrich. 1994*a*. *Shaker* potassium channel gating. II Transitions in the activation pathway. *J. Gen. Physiol.* 103:279–319.

Zagotta, W.N., T. Hoshi, and R.W. Aldrich. 1994*b*. *Shaker* potassium channel gating. III Evaluation of kinetic models for activation. *J. Gen. Physiol.* 103:321–362.